

Scattering Mechanisms in a High Mobility Low Density Carbon-Doped (100) GaAs Two-Dimensional Hole System

J. D. Watson¹, S. Mondal¹, G. A. Csáthy¹, M. J. Manfra^{1,2,3,*},

E. H. Hwang⁴, S. Das Sarma⁴, L. N. Pfeiffer⁵, K. W. West⁵

¹ *Department of Physics and Birck Nanotechnology Center*

² *School of Electrical and Computer Engineering*

³ *School of Materials Engineering*

Purdue University, West Lafayette, IN 47907

⁴ *Condensed Matter Theory Center and Department of Physics*

University of Maryland, College Park, MD, 20742

⁵ *Department of Electrical Engineering*

Princeton University, Princeton, NJ 08544

We report on a systematic study of the density dependence of mobility in a low-density Carbon-doped (100) GaAs two-dimensional hole system (2DHS). At $T=50$ mK, a mobility of 2.6×10^6 cm^2/Vs at a density $p=6.2 \times 10^{10}$ cm^{-2} was measured. This is the highest mobility reported for a 2DHS to date. Using a back-gated sample geometry, the density dependence of mobility was studied from 2.8×10^{10} cm^{-2} to 1×10^{11} cm^{-2} . The mobility vs. density cannot be fit to a power law dependence of the form $\mu \sim p^\alpha$ using a single exponent α . Our data indicate a continuous evolution of the power law with α ranging from ~ 0.7 at high density and increasing to ~ 1.7 at the lowest densities measured. Calculations specific to our structure indicate a crossover of the dominant scattering mechanism from uniform background impurity scattering at high density to remote ionized impurity scattering at low densities. This is the first observation of a carrier density-induced transition from background impurity dominated to remote dopant dominated transport in a single sample.

The two-dimensional hole system (2DHS) offers an attractive platform for the study of strong carrier interactions parameterized by r_s : the ratio of the Coulomb energy to the Fermi energy. $r_s = E_c/E_f \propto m^*/\sqrt{p}$, where p is the hole density and m^* is the effective mass. Recent developments in the growth of Carbon-doped (100) GaAs heterostructures by molecular beam epitaxy (MBE) have resulted in 2DHSs of unprecedented quality^{1,2}. Such structures have been utilized in the study the metal-to-insulator transition (MIT)³, fractional quantum Hall physics in the 2nd Landau level (LL)⁴, spin-orbit coupling in Aharonov Bohm rings⁵ and charge density wave formation in partially filled LL's^{6,7}. These initial experiments and the prospect of studying strong correlations in the presence of tunable spin-orbit coupling provide strong motivation to understand the scattering processes presently limiting mobility in the highest quality samples. Here we present mobility vs. density data on an unprecedentedly high mobility 2DHS. One of the most exciting avenues for future research is the investigation of ultra-low density 2DHSs at very large r_s . Thus, our data and calculations will inform the design of new hole heterostructures of ever increasing quality.

Carbon doping² of 2DHSs offers advantages over the more commonly used acceptor dopants Beryllium and Silicon. Carbon diffuses and surface segregates much less at typical MBE growth temperatures ($T \sim 630$ °C) than

Beryllium⁸. Additionally Carbon can be incorporated as an acceptor on multiple crystallographic orientations, including on the high-symmetry (100) face of GaAs. Silicon can also act as an acceptor to produce high quality 2DHSs but so far high mobility ($\mu \sim 10^6$ cm^2/Vs) Silicon-doped 2DHSs have only been realized on (311)A face⁹. The (311)A face has a well known mobility anisotropy between the $[233]$ and $[01\bar{1}]$ directions⁹ whereas Carbon-doped structures on the (100) face have a significantly lower anisotropy between the $[011]$ and $[0\bar{1}1]$ directions². Furthermore, the high symmetry of the (100) orientation dramatically alters the nature of spin-orbit interactions in 2DHSs as compared to quantization along the (311)A direction. Indeed, further experimental work is needed to fully exploit the potential benefits of Carbon-doped (100) 2DHSs.

Our sample consists of a 20 nm $\text{Al}_{0.16}\text{Ga}_{0.84}\text{As}/\text{GaAs}/\text{Al}_{0.16}\text{Ga}_{0.84}\text{As}$ quantum well asymmetrically modulation doped with Carbon at a density of 1×10^{12} cm^{-2} above the quantum well at a setback of 80 nm. FIG. 1 shows a sketch of the device along with the numerically calculated¹⁰ band structure and heavy hole ground state wavefunction (normalized to unity). For simplicity in simulation the superlattice and buffer regions are truncated. In order to modulate the density in the quantum well, we utilized a back-gate geometry. The sample was first thinned to approximately 150 μm and then cleaved into a Hall bar approximately 2 mm \times 9 mm. Ohmic contacts consist of In/Zn dots positioned approximately 1 mm apart along the length of the Hall bar and annealed at $T =$

*mmanfra@purdue.edu

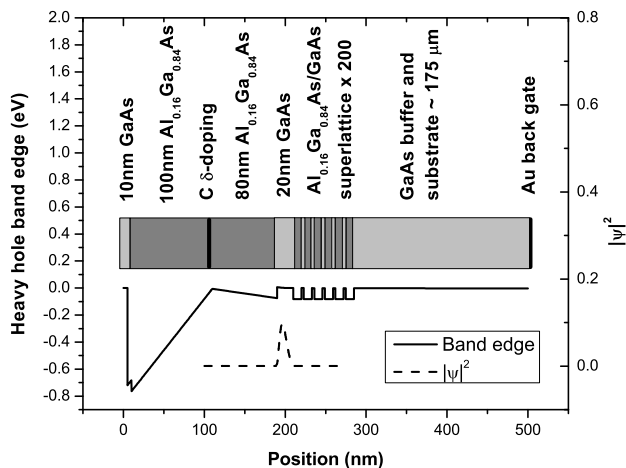


FIG. 1: Schematic of the device structure used in our experiments.

430 °C. The hall bar was subsequently fixed to a gold backgate evaporated on an undoped GaAs substrate. The carrier density was measured from minima in the longitudinal magnetoresistance, and the conductivity was obtained from four-terminal zero field measurements using standard lock-in techniques. As shown in FIG. 2, the 2DHS density depended linearly on voltage over the range measured. Modeling the structure as a parallel plate capacitor with one plate being the 2DHS and the other being the backgate we estimate the gate to be situated 175 μm from the well. The peak mobility μ at low temperature ($T = 50$ mK) was measured to be 2.6×10^6 cm^2/Vs at a density of 6.2×10^{10} cm^{-2} in an as-grown sample.

FIG. 2 also shows the leakage current as a function of the gate voltage. The linear dependence of the leakage current on the gate voltage and its small magnitude (< 1.5 nA as compared to an excitation current of 50 nA) suggest that the observed leakage represents par-

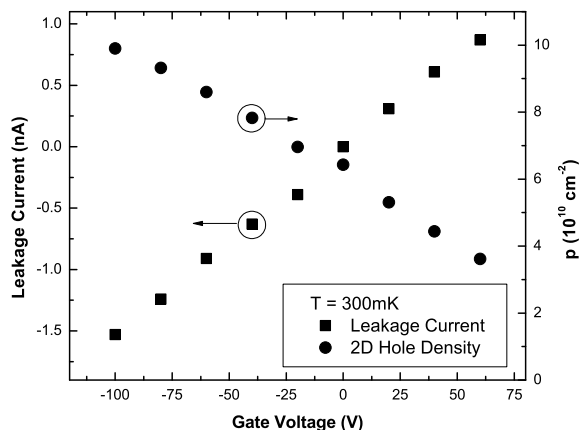


FIG. 2: Effect of gate voltage on carrier density and leakage current at $T = 300$ mK.

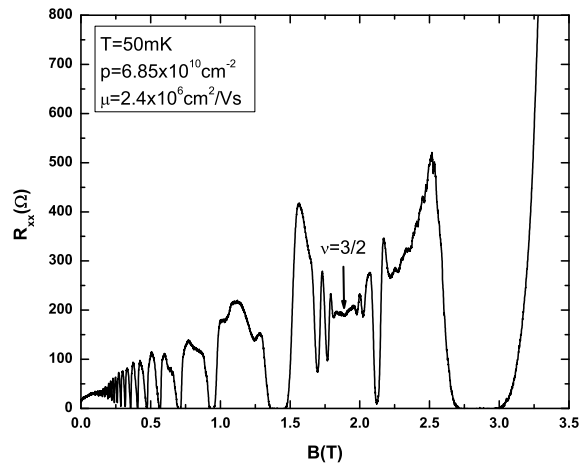


FIG. 3: Low field magnetoresistance of the backgated sample at $T = 50$ mK.

asitic current passing through the measurement circuit and not hard breakdown in the GaAs. In addition, the linear dependence of the density on the gate voltage also suggests that sharp breakdown did not occur. FIG. 3 shows a representative trace of the magnetoresistance at $T = 50$ mK. The deep minima in the fractional quantum Hall states around filling factor $\nu = \frac{3}{2}$ illustrate the high quality of the processed sample. We note that this sample has also been studied at ultra-low temperatures ($T \leq 10$ mK) in which the first evidence of a fully formed fractional quantum Hall state at $\nu = 8/3$ in the 2nd Landau level in a 2DHS was observed⁴.

In order to examine the scattering mechanisms limiting mobility in our system, we measured the dependence of the mobility on the 2D hole density modulated by the backgate as shown in FIG. 4. As can be clearly seen on this log-log plot the data points do not fall on a straight line as would be expected for a single dominant scattering mechanism. The mobility vs. density cannot be fit to a power law dependence of the form $\mu \sim p^\alpha$ using a single exponent α . Our data indicate a continuous evolution of the power law with α ranging from ~ 0.7 at high density and increasing to ~ 1.7 at the lowest densities measured. Thus the data indicate the presence of multiple dominant scattering mechanisms over the range of density tested. Indeed at the lowest densities measured, the mobility decreases rapidly indicating that the system will eventually approach a finite density MIT³. We emphasize, however, that $k_F l$, the product of the Fermi wavevector and the mean free path, remains larger than 50 over the entire range of density tested. It can be seen at high density that the mobility follows a power law behavior $\mu \propto p^{0.7}$ which is indicative of uniformly distributed charged background impurity (BI) scattering^{11,12} in 2D carrier systems. However, the power law continuously shifts towards higher α of approximately 1.7 at low density. Typically, an exponent $\sim 1.5 - 1.7$ is taken as an indication of the dominance of remote ionized (RI) im-

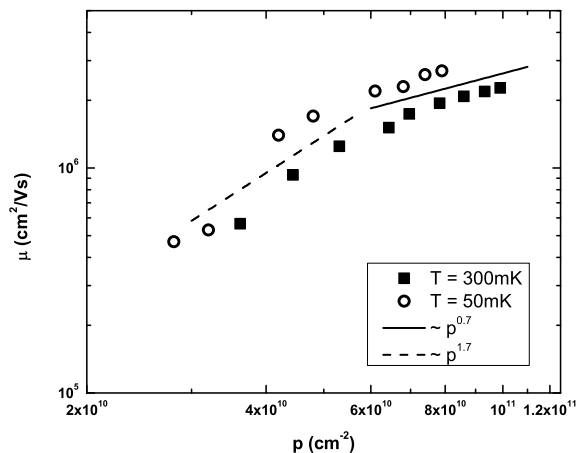


FIG. 4: Mobility as a function of the density at $T = 300$ mK (squares) and $T = 50$ mK (open circles). Straight lines are guides to the eye to the 300 mK data to illustrate 0.7 and 1.7 power laws.

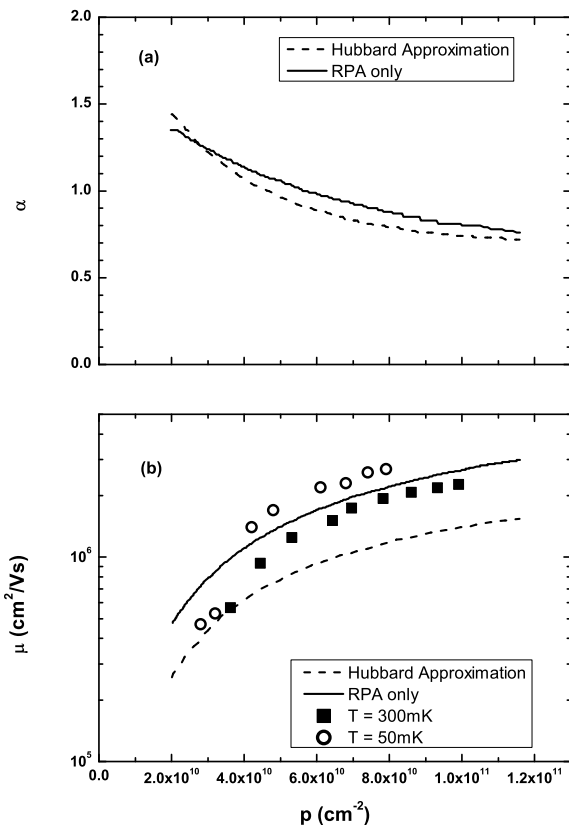


FIG. 5: (a) Theoretical density dependence of the exponent α in $\mu \propto p^\alpha$. (b) Comparison of experimental mobility data and theoretical results. Solid line represents RPA-Boltzmann calculation and dashed line represents RPA-Boltzmann calculation with the Hubbard approximation in both plots.

purity scattering^{11,13} originating in the remote doping layer in 2D systems. We emphasize that it is unusual that such a crossover behavior can be seen in a single

sample while remaining in the high mobility (or equivalently large $k_F l$) regime. It is interesting to note that our setback distance is 80 nm, a distance at which remote ionized impurity scattering usually makes a relatively minor contribution to the total scattering in samples with density $\gtrsim 10^{11}$ cm⁻². Nevertheless, it is clear that for the material parameters of our structure it dominates scattering at lower density. A similar transition to remote ionized impurity scattering in low density 2D electron samples was reported by Jiang et al.¹⁴, but in these samples $k_F l$ was substantially lower and the samples were approaching a conduction threshold. Unusual transport behavior was also recently reported in the 2DHS in an undoped electron-hole bilayer¹⁵ and subsequently explained by carrier inhomogeneities resulting from strong carrier-carrier interactions and non-linear screening¹⁶. It could be argued that $T = 300$ mK data is only marginally outside the range where phonons could be playing some role, but the fact that our $T = 50$ mK data displays the same functional dependence seems to rule out any critical scattering contributions from phonons. Interface roughness (IR) scattering should also be considered, but significant IR scattering should also manifest itself in a significant mobility anisotropy¹² which was not observed in our sample. Finally, scattering between the light and heavy hole bands¹ as well as changes in the effective mass¹⁷ have also been reported. However, both of these effects should decrease as the density is lowered and the Fermi level moves towards the top of the valence band and away from light hole band.

To explain our experimental observation we calculated the Coulomb scattering rate due to background charged impurity scattering and remote charged impurity scattering using a Boltzmann transport method^{18,19}. Screening was taken into account using the random phase approximation (RPA). The calculation was performed both with and without the inclusion of correlation effects via the Hubbard approximation. The analysis assumed a 3D background impurity concentration of $n_{i3D} = 3 \times 10^{13}$ cm⁻³, dopant setback from the center of the quantum well $d = 90$ nm, hole effective mass $m^* = 0.4m_e$ where m_e is the free electron mass, quantum well width $a = 20$ nm, and a remote ionized impurity concentration $n_i = 2 \times 10^{11}$ cm⁻². FIG. 5(a) shows a crossover of the mobility exponent changing from $\alpha \sim 0.7 - 0.8$ to $\alpha \sim 1.5 - 1.7$ which has the same qualitative behavior as seen in the data in FIG. 4. The results of the calculations are compared with the experimental data in FIG. 5(b). Qualitatively, as the hole density is lowered, screening of the remote dopants by the 2D hole gas becomes less effective, and the dominant scattering mechanism transitions from being dominated by uniform background impurities to being dominated by remote dopants. Such a transition point in the density is governed entirely by n_{i3D} , d , and n_i , and thus it is not surprising that this is the first time (to our knowledge) that such a transition has been observed in a single sample within the high mobility regime.

To understand the transition in the transport mech-

anism observed in our data, it is important to realize¹⁶ that the impurity scattering strength in the transport theory carries the form-factor $\exp(-2k_F d)$ at low temperatures where $2k_F$ is the typical momentum transfer for resistive scattering by impurities, and d is the typical separation of the impurities from the 2D carrier layer. Since $k_F \sim p^{1/2}$, it is clear that lowering the carrier density would lead to stronger scattering by remote impurities which is exponentially suppressed at higher values of $k_F d$. For a screened Coulomb potential with two impurity contributions (remote and background charged impurity) we can derive the approximate qualitative formula for the mobility

$$\mu \propto \frac{(k_F d)^3 q_{TF}}{n_i + A n_{i3D} (k_F d)^3 q_{TF} / (2k_F + q_{TF})^2} \quad (1)$$

where A is a density independent constant and $q_{TF} = 2/a_B$ is the Thomas Fermi screening wave vector with the effective Bohr radius $a_B = \hbar^2/m^*e^2$. In the high-density limit, $k_F d \gg 1$ the mobility is proportional to the square of the sum of two wave vectors, i.e., $\mu \propto (2k_F + q_{TF})^2$. However, as $k_F d$ (or, density) decreases the mobility behaves approximately $\mu \propto (k_F d)^3$. Thus, as long as strong localization does not set in, which is the usual situation for lower mobility samples¹⁴, lowering carrier density should always lead to a continuous increase of the exponent α as scattering from the remote dopant impurities becomes important. This is exactly the theoretical behavior predicted in the theory (Fig. 4), and experi-

mentally observed in our extremely high-mobility hole sample.

In conclusion, we measured the density dependence of mobility in a very high quality 2DHS. The 50 mK mobility was found to be 2.6×10^6 cm²/Vs at a density of 6.2×10^{10} cm⁻² in a pristine sample. The mobility appears to be limited by background charged impurity scattering at high density but in the low density regime is a stronger function of the density indicating an increasingly important scattering contribution from remote impurities. From this data, we can surmise that increased 2DHS mobility can be realized at low density by significantly increasing the spacer thickness. Such experiments are currently underway. Our work also demonstrates that in samples of sufficiently high quality, where the 2D MIT transition is pushed down to very low carrier densities, the theoretically predicted continuous transition from background impurity scattering limited transport to remote dopant scattering limited transport can be quantitatively verified by decreasing the carrier density in a single sample.

Acknowledgment

JDW is supported by a Sandia Laboratories/Purdue University Excellence in Science and Engineering Fellowship. MJM acknowledges support from the Miller Family Foundation. The work by Maryland (EH and SDS) is supported by Microsoft Q. GAC acknowledges support from the NSF DMR-0907172.

-
- ¹ C. Gerl, S. Schmult, H.-P. Tranitz, C. Mitzkus, and W. Wegscheider, *Appl. Phys. Lett.* **86**, 252105 (2005).
 - ² M. J. Manfra, L. N. Pfeiffer, K. W. West, R. de Picciotto, and K. W. Baldwin, *Appl. Phys. Lett.* **86**, 162106 (2005).
 - ³ M. J. Manfra, E. H. Hwang, S. Das Sarma, L. N. Pfeiffer, K. W. West, and A. M. Sergent, *Phys. Rev. Lett.* **99**, 236402 (2007).
 - ⁴ A. Kumar, N. Samkharadze, M. J. Manfra, G. A. Csáthy, L. N. Pfeiffer, K. W. West, arXiv:1007.1504v1 (2010).
 - ⁵ B. Grbić, R. Leturcq, T. Ihn, K. Ensslin, D. Reuter, and A. D. Wieck, *Phys. Rev. Lett.* **99**, 176803 (2007).
 - ⁶ S. P. Koduvayur, Y. Lyanda-Geller, S. Khlebnikov, G. Csáthy, M. J. Manfra, L. N. Pfeiffer, K. W. West, and L. P. Rokhinson, *Phys. Rev. Lett.* **106**, 016804 (2011).
 - ⁷ M. J. Manfra, R. de Picciotto, Z. Jiang, S. H. Simon, L. N. Pfeiffer, K. W. West, and A. M. Sergent, *Phys. Rev. Lett.* **98**, 206804 (2007).
 - ⁸ E. F. Schubert, *Doping in III-V Semiconductors* (Cambridge University Press, Cambridge, 1993).
 - ⁹ J. J. Heremans, M. B. Santos, K. Hirakawa, and M. Shayegan, *J. Appl. Phys.* **76**, 1980 (1994).

- ¹⁰ Nextnano3 simulator ©1999-2008 Walter Schottky Institute. <http://www.nextnano.de/nextnano3/index.htm>.
- ¹¹ E. H. Hwang and S. Das Sarma, *Phys. Rev. B* **77**, 235437 (2008).
- ¹² V. Umansky, R. de Picciotto, and M. Heiblum, *Appl. Phys. Lett.* **71**, 683 (1997).
- ¹³ K. Lee, M. S. Shur, T. J. Drummond, and H. Morkoç, *J. Appl. Phys.* **54**, 6432 (1983).
- ¹⁴ C. Jiang, D. C. Tsui, and G. Weimann, *Appl. Phys. Lett.* **53**, 1533 (1988).
- ¹⁵ J. A. Seamons, D. R. Tibbetts, J. L. Reno, and M. P. Lilly, *Appl. Phys. Lett.* **90**, 052103 (2007).
- ¹⁶ E. H. Hwang and S. Das Sarma, *Phys. Rev. B* **78**, 075430 (2008).
- ¹⁷ T. M. Lu, Z. F. Li, D. C. Tsui, M. J. Manfra, L. N. Pfeiffer, and K. W. West, *Appl. Phys. Lett.* **92**, 012109 (2008).
- ¹⁸ S. Das Sarma and E. H. Hwang, *Phys. Rev. Lett.* **83**, 164 (1999).
- ¹⁹ S. Das Sarma and E. H. Hwang, *Phys. Rev. B* **61**, 7838 (2000).